Fault detection and isolation using Multiple model parameter estimation

Philippe Weber, Sylviane Gentil

WEBER P., GENTIL S.: Fault detection and isolation using Multiple model parameter estimation. CESA'98 IMACS, Multiconference, Computational Engineering in Systems Applications, Vol.3, pp 467-472, Nabeul-Hammamet, Tunisia, Apr. 1-4, 1998

Fault Detection and Isolation using Multiple Model Parameter Estimation

P. WEBER, S. GENTIL
Laboratoire d'Automatique de Grenoble UMR-CNRS 5528-UJF
E.N.S.I.E.G., BP 46, 38402 Saint Martin d'Hères Cedex - France
weber@lag.ensieg.inpg.fr, gentil@lag.ensieg.inpg.fr
Phone: (33) 4 76 82 63 85
Fax: (33) 4 76 82 63 88

ABSTRACT

On line parameter estimation reflects the process state, but physical parameters are not usually easily estimated in the case of complex systems. This paper presents a sensor or actuator fault detection method based on a classical transfer function parameter estimation algorithm in discrete time domain. Redundant discrete time transfer functions are used to improve the residual generation. The increase of information by redundant equations allows the generation of a signature table. The fault detection and isolation (FDI) is achieved by the exploitation of this table, with a distance computation.

Keywords: Fault detection, diagnosis and isolation; parameter estimation; actuator and sensor faults; fuzzy decision making.

1. INTRODUCTION

During the last two decades many fault diagnosis methods based on dynamic models have appeared in response to the increasing complexity of process supervision [4]. Such methods are generally based on:

- state estimation [9],
- parity space and parity relations [2],
- parameter estimation [5],
- causal graphs [8].

On line parameter estimation reflects the process state and therefore might allow FDI. For not too complex processes, continuous time parameter estimation makes it possible to come back to physical parameters [5]. A direct knowledge of the different system elements simplifies the fault diagnosis task. Nevertheless, it is very difficult to obtain the physical model of a complex process, because physical parameters are not usually precisely known. The aim of this work is to test classical parameter estimation methods as a diagnosis tool. Classical estimation methods are well known, and can be found in the control engineer's toolboxes. In this case, using discrete transfer function representation, the parameters cannot be linked directly to physical properties, and the parameter estimation is followed by a classification technique in order to achieve the FDI.

This paper is organised as follows: section two presents briefly the winding system that has been used as application; in the section three the symptom generation technique is proposed. Extended Least Square estimation of a reference model and a tracking model allows the residual generation. Afterwards, residual fuzzification is detailed as a residual evaluation task, and fuzzy aggregation leads to the symptom generation. Section four presents the redundant transfer function generation which allows the elaboration of the signature table and fault isolation technique using distance computation. Finally, the application results on the winding system simulation are presented and commented in section five, before concluding remarks.

2. THE WINDING SYSTEM MODEL

The approach presented in this paper has been applied to the pilot plant represented in figure 1. This winding system is composed by three DC-motors (M_1, M_2, M_3). Their angular velocities are represented by Ω_1, Ω_2 and Ω_3, which are respectively controlled by u_1, u_2 and u_3. The angular velocity Ω_2, and the strip tensions T_1 and T_3 between the reels are measured respectively by tachometers and tension-meters. The angular velocities Ω_1, Ω_3 are not measured.

The model can be written as a linear discrete state representation where Ω_i, i=1, 2, 3, and T_1, T_3 are the state variables [3] as follows:

$$T_1(k)=a_{T1}.T_1(k-1)+b_{T1v2}.\Omega_2(k-1)+b_{T1v1}.\Omega_1(k-1) \quad (1)$$

$$\Omega_2(k)=a_{v2}.\Omega_2(k-1)+b_{v2T1}.T_1(k-1)+b_{v2T3}.T_3(k-1)+ b_{v2u2}.u_2(k-1) \quad (2)$$

$$T_3(k)=a_{T3}.T_3(k-1)+b_{T3v2}.\ \Omega_2(k-1)+b_{T3v3}.\ \Omega_3(k-1) \quad (3)$$

$$\Omega_3(k)=a_{v3}.\Omega_3(k-1)+b_{v3T3}.T_3(k-1)+b_{v3u3}.u_3(k-1) \quad (4)$$

$$\Omega_1(k)=a_{v1}.\Omega_1(k-1)+b_{v1T1}.T_1(k-1)+b_{v1u1}.u_1(k-1) \quad (5)$$

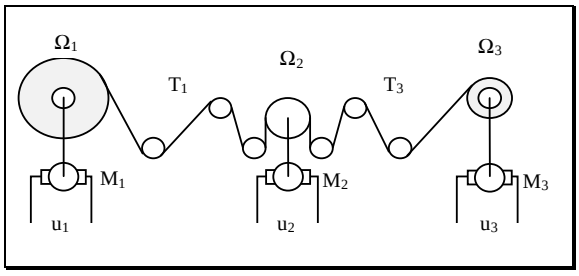

Figure 1: Winding system.

The parameters a_{ij} and b_{ij} are not known a priori. In a transfer function representation, putting (5) into (1) and (4) into (3) allows to eliminate the state variables Ω_1 and Ω_3 which are not measurable. A parameter estimation allows to conclude that the gains of the transfer functions relating Ω_2 to T_1 and to T_3 are

negligible. Three simplified input-output models are thus defined as follows:

$$A_1(q^{-1}).T_1(k)=B_{12}(q^{-1}).\Omega_2(k-d_{12})+B_{1u1}(q^{-1}).u_1(k-d_{1u1}) \quad (6)$$

$$A_2(q^{-1}).\Omega_2(k)= B_{2u2}(q^{-1}).u_2(k-d_{2u2}) \quad (7)$$

$$A_3(q^{-1}).T_3(k)=B_{32}(q^{-1}).\Omega_2(k-d_{32})+B_{3u3}(q^{-1}).u_3(k-d_{3u3}) \quad (8)$$

3. SYMPTOM GENERATION

Parameter estimation

Using AutoRegressive Moving Average with eXternal input (ARMAX) structure, parameters of equations (6), (7) and (8) can be estimated by Extended Least Square (ELS) algorithm [7].

An on-line parameter estimation with a long time horizon estimator allows to follow the slow variations of the parameters. This kind of variations are not considered as faults, but caused by the ageing of the process. For the winding system example, the reel inertia is a function of reel diameter, thus winding system is a time varying parameter system with slow variations. The long horizon estimates are computed by an on-line ELS algorithm with a forgetting factor equal to 1. This algorithm results in a reference model parameter estimate vector Es_h^l of the model h (h=1...3) (eq. (9)).

$$Es_h^l = \left[\Theta_1^h \quad ... \quad \Theta_{p^h}^h \right] \quad (9)$$

where p^h is the number of parameters for each model h.

A second estimator based on a short time horizon, allows to follow fast variations considered as symptoms of a fault. This estimator allows the estimation of the tracking model [1]. The short horizon estimator is computed by the same ELS algorithm with, initially, a smaller forgetting factor, and produces the tracking model parameter estimate vector Es_h^s of the model h (eq. (10)). The tracking capability depends on this initial forgetting factor choice.

$$Es_h^s = \left[\theta_1^h \quad ... \quad \theta_{p^h}^h \right] \quad (10)$$

The algorithm used to achieve the different estimations is computed by orthogonal transformation that allows good numerical properties [10].

In order to avoid the problems due to non persistent excitation, the forgetting factors of the tracking model estimators are adapted on line in relation with the *condition number* and the *prediction error*.

- A c*ondition number* increase means that the excitation is poor. In this case the forgetting factor is increased to one.
- A *prediction error* increase means a discrepancy between the system and the model. This situation is classically the symptom of a fault. In this case, the forgetting factor is changed to the initial forgetting factor.

Residual generation

The residuals are computed by the difference between the long horizon estimates Θ_j^h and the short horizon estimates θ_j^h :

$$r_j^h = \Theta_j^h - \theta_j^h \quad (11)$$

The residual mean is:

$$\rho_{rj} = \rho_{\Theta j} - \rho_{\theta j} \quad (12)$$

If no fault occurs the residual mean should be close to zero, because ELS algorithm allows non biased parameter estimation. But the residual variance depends on correlation hypotheses. If estimates are not correlated (the faulty case) the variance is defined by:

$$\sigma_{rj}^{\ 2} = \sigma_{\Theta j}^{\ 2} + \sigma_{\theta j}^{\ 2}, \quad (13)$$

and in the case of a correlation between Θ_j and θ_j , (the fault free case) residual variance is computed by:

$$\sigma_{rj}^{\ 2} = \sigma_{\Theta j}^{\ 2} + \sigma_{\theta j}^{\ 2} - 2 \cdot \mathrm{E}\left\{\Theta_j^* \cdot \theta_j^*\right\} \quad (14)$$
$$\sigma_{rj}^{\ 2} \geq \left(\sigma_{\Theta j} - \sigma_{\theta j}\right)^2$$

where Θ_j^* and θ_j^* represent the centered estimates.

Thus the residual variance is bounded by (13) and (14). When the residual is close to zero, the residual variance is close to (14) and if the residual is positive then the residual variance is close to (13).

Residual fuzzification

In order to bypass the unknown residual probability distribution, fuzzy set theory is used [11].

Two fuzzy sets are defined in $\Re_+$ the universe of discourse of absolute values of residuals r_j^h ; Z for ZERO, and P for POSITIVE. The fuzzy set Z is the complement of P (Figure 2).

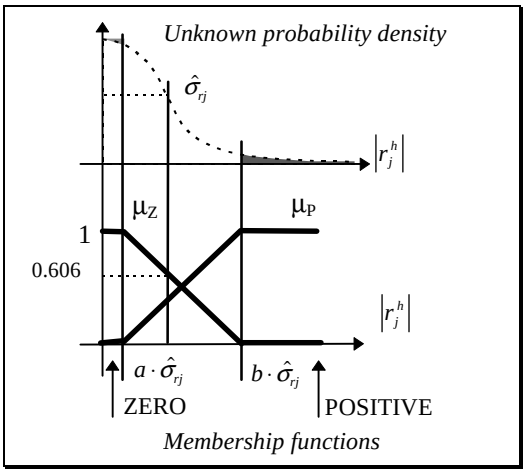

Figure 2: Residual fuzzification.

The membership functions are dynamically adapted to the residual variance which is chosen by linear interpolation between the equations (13) and (14), depending on the POSITIVE membership degree computed at the previous step.

$$\tilde{\sigma}_{rj}^2(k) = (\sigma_{\Theta j}(k) - \sigma_{\theta j}(k))^2 - \mu_P(|r_j(k-1)|) \cdot \left\{(\sigma_{\Theta j}(k) - \sigma_{\theta j}(k))^2 - (\sigma_{\Theta j}^2(k) + \sigma_{\theta j}^2(k))\right\} \quad (15)$$

Thus the membership functions to the two sets are defined by:

$$\mu_P(|r_j(k)|) = \min\left(1, \max\left(0, \frac{|r_j(k)| - a \cdot \hat{\sigma}_{r_j}(k)}{b \cdot \hat{\sigma}_{r_j}(k) - a \cdot \hat{\sigma}_{r_j}(k)}\right)\right) \quad (16)$$

$$\mu_Z(|r_j(k)|) = 1 - \mu_P(|r_j(k)|)$$

where a and b are chosen to tune sensitivity (for trapezoidal approximation of a gaussian function, a=0.35 and b=2).

Aggregation

For actuator or sensor fault detection and isolation, the relevant information is a *global perturbation* of all parameter estimates Es_h^s. Note that estimate vectors (Es_h^s) have not necessarily the same dimension.

Thus a global perturbation degree is computed for each vector Es_h^s, using residual membership degrees to the fuzzy sets. The symptom vector s_h representing the state of the model h, is defined on the universe $\Re_+^{p^h}$ which is the cartesian product of the residual universes of discourse, where p^h is the dimension of Es_h^s.

$$s_h = [|r_1^h| \quad ... \quad |r_{p^h}^h|] \quad \text{where } s_h \in \Re_+^{p^h} \quad (17)$$

Two fuzzy sets are defined on the $\Re_+^{p^h}$ universe: Globally Perturbed (GP) and Not Perturbed (NP). The membership degrees of s_h to the sets GP and NP are computed by aggregation techniques of the residual fuzzy descriptions.

Several kinds of aggregation functions can be proposed [11]. A T-norm aggregation is not enough sensitive because if one of the elements is near to zero then the aggregation result is near to zero. A T-conorm aggregation is very sensitive because if just one elements is near to one, then the result will be near to one. Thus T-norm and T-conorm are not suitable operators. A mean aggregation operator seems to be a good compromise between a T-norm and a T-conorm.

Membership functions to GP and NP sets are thus defined by:

$$\mu_{GP}(s_h) = \frac{1}{p^h}\sum_{j=1}^{p^h} \mu_P(|r_j^h|) \quad (18)$$

$$\mu_{NP}(s_h) = 1 - \mu_{GP}(s_h)$$

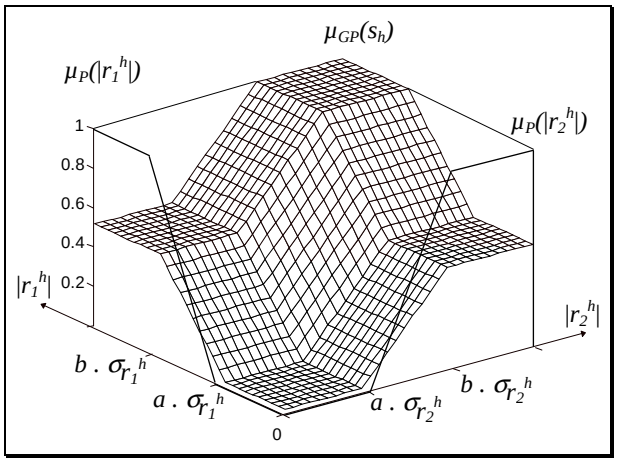

Figure 3: GP membership function (2D example).

As an example Figure 3 represents GP membership function, using just two residuals $|r_1^h|$ and $|r_2^h|$. This membership function is defined on $\Re_+^2$ universe, and computed by (18).

4. FAULT ISOLATION USING REDUNDANT TRANSFER FUNCTION

Signature table generation

When a sensor or actuator fault like a bias occurs, all the estimates of a model sensitive to the fault, are perturbed due to the ARMAX structure. Thus, only the transfer functions uncoupled to the faulty measurements or inputs can be estimated without perturbation of their parameters.

In a signature table called $D_1(n,h)$ (or diagnostic matrix [6]) the vectors of estimates Es_h^s perturbed by a fault are represented by '1', and those not affected are represented by '0'. H columns are linked to models h (H=3 in D_1). The rows represent the fault signatures respectively for a fault in T_1, Ω_2, T_3, u_1, u_2, and u_3. Each fault signature is a binary vector noted Sg_n, (Table 1).

D_1	Es_1^s	Es_2^s	Es_3^s
Sg_{T1}	1	0	0
$Sg_{\Omega 2}$	1	1	1
Sg_{T3}	0	0	1
Sg_{u1}	**1**	**0**	**0**
Sg_{u2}	**0**	**1**	**0**
Sg_{u3}	**0**	**0**	**1**

Table 1

As shown in table 1, the signature of a fault on Ω_2 ($Sg_{\Omega 2}$) includes all other signatures. This occurs a problem for the isolation of simultaneous faults. But for actuator faults, table 1 shows good isolation property (Sg_{u1}, Sg_{u2} and Sg_{u3}).

The use of additional transfer function estimation allows to extend the signature table 1, by adding new symptoms. It can be done using eq. (6), (7) and (8) as parity relations [3]. Putting eq. (7) into (6) a model that links T_1 to u_1 and u_2 is obtained; with this model, T_1 and Ω_2 are no more coupled. The parameters estimated in this way will not be sensitive to the faults on Ω_2. The same procedure can be applied for (8) and (7) and so, the vector of estimates Es_4^s and Es_5^s can thus be obtained from:

$$A_{11}(q^{-1}).T_1(k) = B_{11u2}(q^{-1}).u_2(k-d_{11u2}) + B_{11u1}(q^{-1}).u_1(k-d_{1u1}) \quad (19)$$

$$A_{33}(q^{-1}).T_3(k) = B_{33u2}(q^{-1}).u_2(k-d_{33u2}) + B_{33u3}(q^{-1}).u_3(k-d_{3u3}) \quad (20)$$

After off line identification, the gain between T_3 and u_2 (in eq. (20)) is proved to be very small thus equation (20) takes the following form:

$$A_{33}(q^{-1}).T_3(k) = B_{33u2}(q^{-1}).u_2(k-d_{33u2}) + B_{33u3}(q^{-1}).u_3(k-d_{3u3}) \quad (21)$$

The signature table $D_2(n,h)$, is represented in table 2 using the vector of estimates Es_4^s, Es_2^s and Es_5^s. Table 2 shows a well structured sub-matrix to isolate sensor faults.

Thus for actuator fault isolation, table 1 is well appropriated; for sensor fault isolation table 2 is well appropriated. If actuator **and** sensor faults are taken into account, it is interesting to use all transfer functions as it is shown in table 3. Faults on T_1 (T_3) and u_1 (u_3) are unfortunately still not isolated.

D_2	Es_4^s	Es_2^s	Es_5^s
Sg_{T1}	**1**	**0**	**0**
$Sg_{\Omega 2}$	**0**	**1**	**0**
Sg_{T3}	**0**	**0**	**1**
Sg_{u1}	1	0	0
Sg_{u2}	1	1	0
Sg_{u3}	0	0	1

Table 2

D	Es_1^s	Es_2^s	Es_3^s	Es_4^s	Es_5^s
Sg_{T1}	1	0	0	1	0
$Sg_{\Omega 2}$	1	1	1	0	0
Sg_{T3}	0	0	1	0	1
Sg_{u1}	1	0	0	1	0
Sg_{u2}	0	1	0	1	0
Sg_{u3}	0	0	1	0	1

Table 3

Isolation function

The vector S of GP membership degrees is defined as:

$$S = [\mu_{GP}(s_1), \ldots, \mu_{GP}(s_H)] \quad (22)$$

If this vector is close to zero, there is no fault detected. Otherwise a decision procedure will try to isolate the fault.

The isolation function noted $F_I(S, Sg_n)$ is achieved comparing S to the signatures Sg_n. It has to measure the similarity between the fault signatures and S. This similarity can be determined by a distance computation.

Figure 4 gives an example for two models, and three faults. (S vector and fault signatures are represented in a two dimensional space.)

The distance between two vectors $A=[a_1 \ldots a_H]$ and $B=[b_1 \ldots b_H]$ in the H dimensional space $\Im$ takes the general form [11]:

$$\left(\sum_{h=1}^{H} |a_h - b_h|^q\right)^{\frac{1}{q}} \quad (23)$$

where q>0.

if q=1, (23) defines the Hamming distance between *A* and *B*.

Using the complement of the Hamming distance allows the generation of the isolation function $F_I(S, Sg_n)$:

$$F_I(S, Sg_n) = 1 - \frac{1}{H}\sum_{h=1}^{H} |\mu_{GP}(s_h) - D(n,h)| \quad (24)$$

such that $F_I(S, Sg_n) \in [0,1]$.

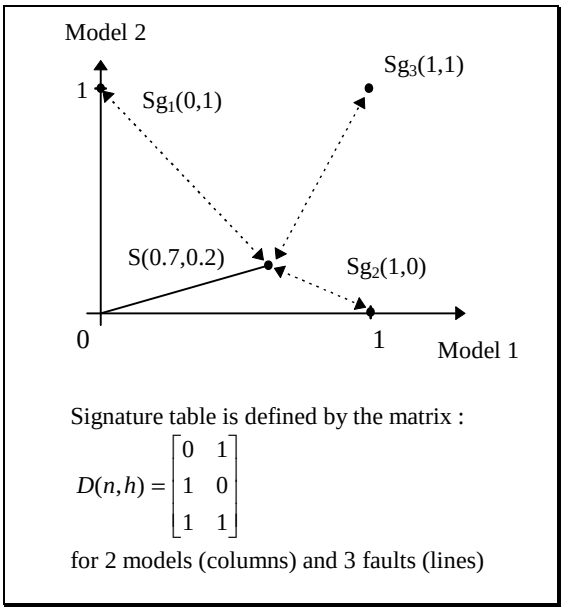

Signature table is defined by the matrix :

$$D(n,h) = \begin{bmatrix} 0 & 1 \\ 1 & 0 \\ 1 & 1 \end{bmatrix}$$

for 2 models (columns) and 3 faults (lines)

Figure 4: Signature representation in the model space.

Considering a fault n, only symptoms s_h corresponding to a "1" in the fault signature vector Sg_n, may be detected as Globally Perturbed and other symptoms must be detected as Not Perturbed. But for simultaneous faults, the vector S is composed by the superposition of the different fault effects. In fact, S must be compared to the logical OR between the different signatures of simultaneous faults. Thus (24) is used only for single fault.

In the multiple fault case, the idea is to calculate the distance between S and Sg_n in a sub-space $\Im'$ excluding insensitive symptoms [10], by excluding dimensions linked to the columns of the fault signature Sg_n which are equal to zero. Thus the isolation function defined by (24) is changed to:

$$F_I(S, Sg_n) = 1 - \frac{1}{W_n}\sum_{h=1}^{H} \{|\mu_{GP}(s_h) - D(n,h)| . D(n,h)\} \quad (25)$$

where W_n is the number of elements $D(n,h) \neq 0$.

5. APPLICATION

The analysis of the above described method was done with a system simulator and using the redundant signature table (Table 3).

The inputs u_1 u_2 and u_3 are step signals at sample 50, 100 and 150 and the sampling period is equal to 0.1s. The signal to noise ratio was fixed to 31 dB.

Sensor fault

The fault was simulated as a 10 % bias on the sensor Ω_2, at time 300 (Figure 5).

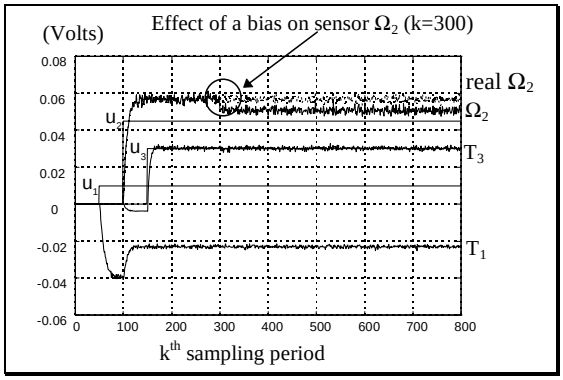

Figure 5: Inputs and measurements around the operating point.

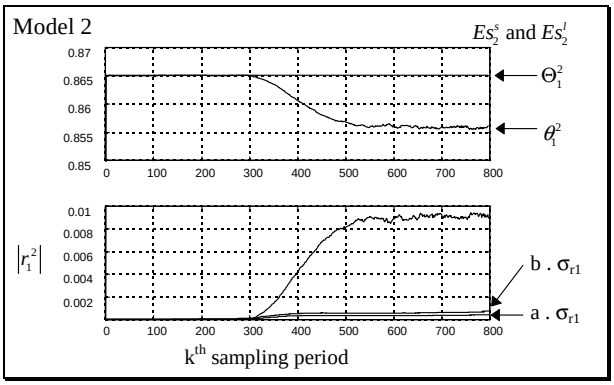

Figure 6: Es_1 estimates and associated residual evolution.

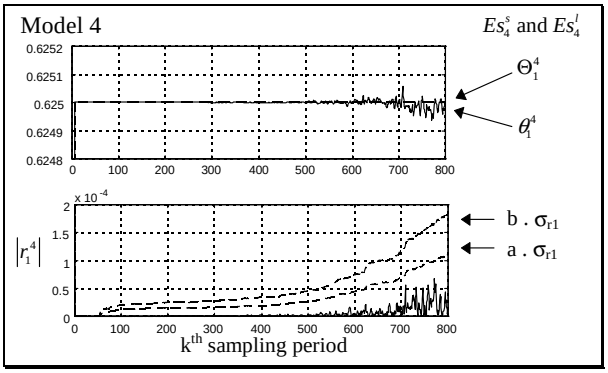

Figure 7: Es_4 estimates and associated residual evolution.

Figure 6 presents the evolution of one of the parameter estimates of the model 2, eq.(7). This estimate is affected by the bias on Ω_2, thus the residual is POSITIVE. Figure 7 presents an estimate of model 4, eq. (19). The short horizon parameter is not affected by the bias on sensor Ω_2 thus the residual is ZERO.

The vector S is computed with the membership degrees to Globally Perturbed of the different models (Figure 8). A comparison between S and the different signatures Sg_n, allows the detection and isolation of the fault. Figure 9 presents the isolation functions related to table 3. $F_I(S,Sg_{\Omega 2})$ (25) is greater than 0.5, 50 sampling periods after the fault occurrence, thus the fault is isolated.

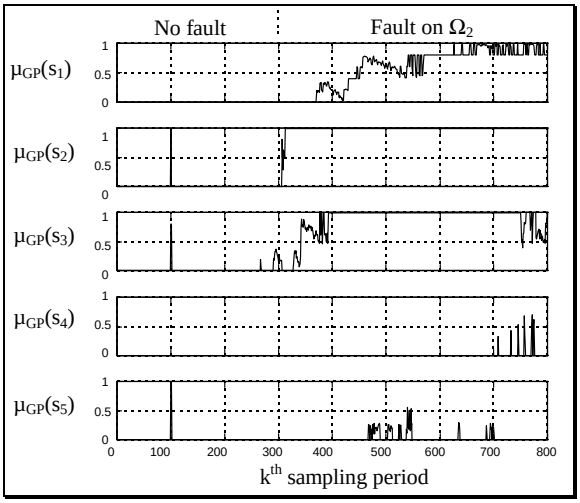

Figure 8: Membership degree of s_h to the sets GP.

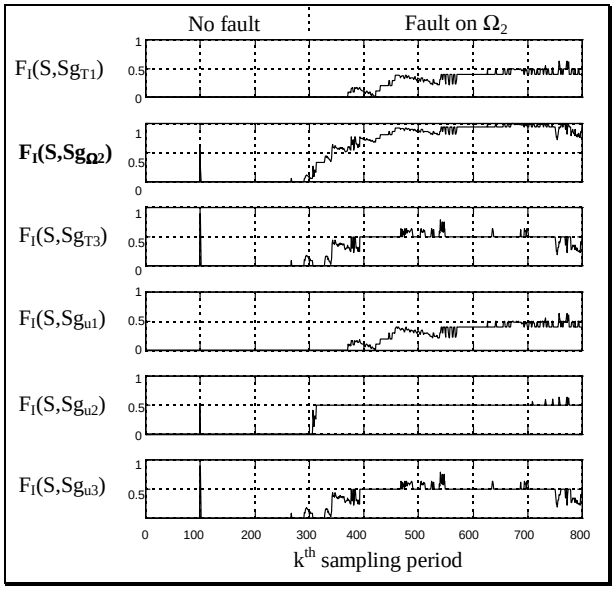

Figure 9: Evolution of the isolation functions for sensor fault.

Actuator fault

The fault was simulated as a 50 % bias on the actuator u_2, at time 300 (Figure 10).

Figure 11 presents the evolution of one of the parameter estimates of model 1, eq. (6). The short horizon parameter is not affected by the bias on actuator u_2. Thus the residual is ZERO. Despite the estimate variance increase after sampling time 400 (caused by non persistent excitation), the residual fuzzification is correct because dynamic membership functions adapted to the estimate variance are used (as explained in section 4). Figure 12 presents a parameter estimate of model 4, eq. (19), this estimate is affected by the bias on u_2, thus the residual is POSITIVE.

Figure 13 presents the isolation functions. Isolation function $F_I(S,Sg_{u2})$ is 0.5, 20 sampling periods after the fault occurrence, thus the fault is quickly isolated. But there are a lot of false detections due to the non persistent excitation.

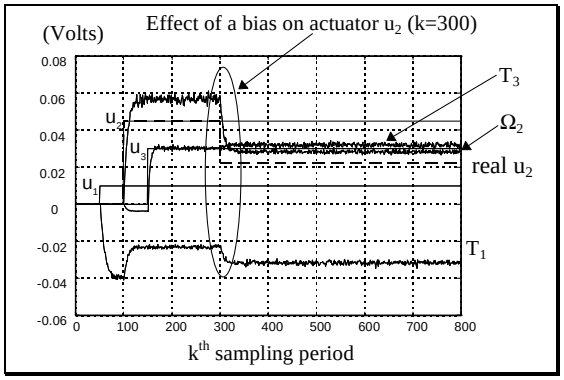

Figure 10: Inputs and measurements around the operating point.

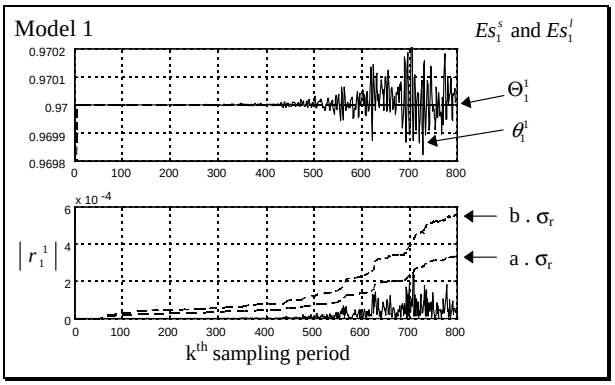

Figure 11: Es_1 estimates and associated residual evolution.

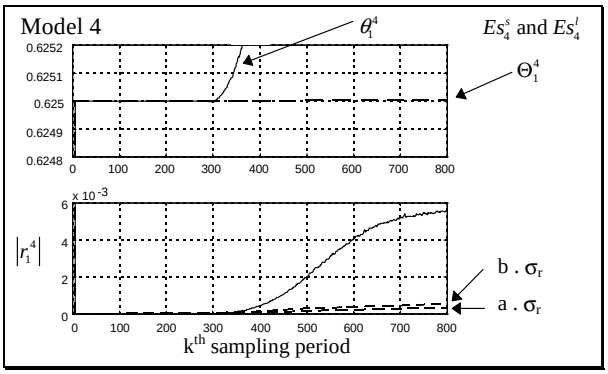

Figure 12: Es_4 estimates and associated residual evolution.

6. CONCLUSION

This paper proposes a method for the fault detection and isolation of a bias on sensors or actuators based on parameter estimation. A classical identification method is used to estimate discrete time transfer function parameters. Several models are used for the same system, linking outputs directly to inputs or to inputs and other outputs. The use of estimates redundancy has allowed the generation of a decision procedure for fault isolation. This decision uses fuzzy sets to support the aggregation of symptoms on each estimated parameter and a Hamming distance for classification of symptoms in the signature space.

Acknowledgements

We thank Dr Sauter and his team, from CRAN (Nancy, France) for providing the model and data of the winding system.

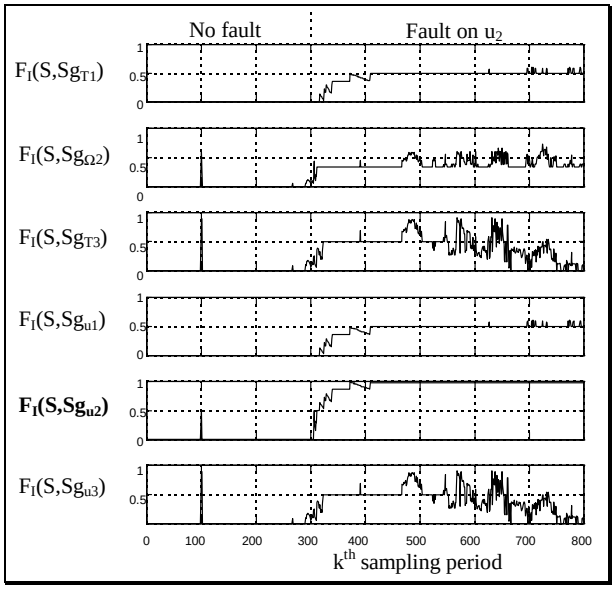

Figure 13: Evolution of the isolation functions for actuator fault.

7. REFERENCES

[1] Basseville M., "Detecting changes in signals and systems - A survey", Automatica, Vol. 24, No. 3, pp. 309-326, 1988.

[2] Gertler J., "Fault detection and isolation using parity relations", Control Eng. Practice, Vol. 5, No. 5, pp. 653-661, 1997.

[3] Hittinger J.-M., "Identification, commande et diagnostic d'un système multivariable d'entraînement de bande", Technical Report CRAN, Nancy - France, 1996.

[4] Isermann R., Ballé P., "Trends in the application of model-based fault detection and diagnosis of technical processes", Control Eng. Practice, Vol. 5, No. 5, pp. 709-719, 1997.

[5] Isermann R., "Fault diagnosis of machines via parameter estimation and knowledge processing - Tutorial paper", Automatica, Vol. 29, No. 4 , pp. 815-835, 1993.

[6] Koscielny J.M., Bartys M.Z., "Smart positioner with fuzzy based fault diagnosis", IFAC Symposium on fault detection supervision and safety for technical processes SAFEPROCESS'97, Vol. 2, pp. 603-608, Kingston Upon Hull, UK, Aug. 26-28, 1997.

[7] Ljung L., "System identification: Theory for the user", Prentice-Hall Englewood Cliffs Information and system science series, New Jersey, 1987.

[8] Montmain J., Leyval L., "Causal graphs for model based diagnosis", IFAC Symposium on fault detection supervision and safety for technical processes SAFEPROCESS'94, Vol. 1, pp. 347-355, Espoo, Finland, Jun. 13-16, 1994.

[9] Patton R.J., Chen J., "Observer-based fault detection and isolation: robustness and application", Control Eng. Practice, Vol. 5, No. 5, pp. 671-682, 1997.

[10] Weber P., Gentil S., "Fault detection using parameter estimation applied to a winding machine", IAR Annual Conference, Duisburg, Germany, Nov. 20-21, 1997.

[11] Yager R.R., Zadeh L.A., "Fuzzy sets, neural networks, and soft computation", Van Nostrand Reinhold, New York, USA, 1994.